

## Lateral distribution of vertical and inclined showers during thunderstorms

---

Lin Chen, KeGu AXi\*, Xunxiu Zhou,\* Daihui Huang, Zhicheng Huang and Peihan Wang

*School of Physical Science and Technology, Southwest Jiaotong University, Chengdu 610031, China*

*E-mail: axkg@my.swjtu.edu.cn, zhouxx@swjtu.edu.cn*

*Abstract.* Ground-based cosmic ray observatories generally record the information on the arrival time and location of each hit to reconstruct the primary direction of the shower event. During thunderstorms, the directions of cosmic rays are changed due to the acceleration and deceleration of the particles when they cross layers of electric field. The thunderstorm field also has a secondary effect on the photons generated via bremsstrahlung, emitted by the high-energy positrons and electrons. So, the lateral distribution of ground cosmic rays could be influenced in thunderstorm electric field. In this work, we performed Monte Carlo simulations by using CORSIKA to study the effects of near-earth thunderstorms electric field on the lateral distribution of vertical and inclined showers at LHAASO (4410 m a. s. 1., Daocheng, China). We found the lateral distribution of secondary positrons, electrons and photons changed in field. The variation amplitude is not only dependent on electric field, but also highly correlated with the direction of the shower event. Our simulation results are useful to understand the acceleration mechanisms of secondary particles caused by an atmospheric electric field, as well as the experimental data obtained by ground-based detectors (such as LHAASO, ARGO-YBJ).

*Keywords:* Near-earth thunderstorms electric field, Lateral distribution, Monte Carlo simulations, Cosmic rays

*37<sup>th</sup> International Cosmic Ray Conference (ICRC 2021)  
July 12th – 23rd, 2021  
Online – Berlin, Germany*

---

\*Presenter

## 1. Introduction

When the high-energy primary cosmic rays enter the atmosphere, they have strong interaction with the atomic nuclei, leading to a large number of secondary particles by hadron and electromagnetic cascades. In the ground-based experiments, there are two common independent data acquisition systems, corresponding to the shower and scaler operation modes. In shower mode, the information on the arrival time and location of each hit are recorded to reconstruct the shower core. Also, we could reconstruct the direction of the primary shower by the time and position of the secondary particles reaching the detector.

The lateral distribution is the density distribution of secondary cosmic rays around the shower axis at observation level [1]. It plays an important role in studying information of primary cosmic rays and the acceleration mechanism. For years, many studies on the lateral distribution of secondary particles in absence of an electric field were carried out [2, 3].

It has been found that the electric field intensity during thunderstorm can be as high as 1000 V/cm or even higher [4]. Wilson proposed that the strong electric field in thunderstorm cloud accelerates the electrons with small mass in secondary cosmic ray to very high energy for the first time [5]. In 1992, Gurevich et al. [6] proposed the relativistic runaway electron avalanche mechanism (RREA). It was believed that the secondary electrons may ionize the air molecules, which results in the avalanche process, and make the electrons grow exponentially under the condition that they get high enough energy through accelerated by the thunderstorm electric field.

The lateral distribution of the positrons and electrons in secondary particles could be influenced by accelerated or decelerate in the thunderstorm electric field. Moreover, the main generation mechanism of photons in extensive air shower is bremsstrahlung. Therefore, the electric field does not act on the photons directly, it still has significant effects on the lateral distribution of photons [7].

The Large High Altitude Air Shower Observatory (LHAASO) located in Daocheng, Sichuan Province, China, is featured with high altitude and frequent thunderstorms in summer [8]. As the main parts of this project, the electromagnetic particle detector (ED) in the kilometer-square array (KM2A) and the water Cherenkov detector array (WCDA) are sensitive to the secondary positrons, electrons and photons in extensive air shower (EAS). In this work, Monte Carlo simulations were performed with CORSIKA to study the effects of near-earth thunderstorms electric field on the lateral distribution of vertical and inclined showers at LHAASO.

## 2. Simulation parameters

CORSIKA is a detailed Monte Carlo program to study the evolution and properties of extensive air showers in the atmosphere [9]. In this work, we simulated the lateral distribution of positrons, electrons and photons for vertical and inclined showers in different fields by CORSIKA 7.5700. The hadronic interactions model is used QGSJETII-04 for the high-energy and GHEISHA for the low energy. The primary particles are protons with energy from 100 GeV to 100 PeV and corresponding to power spectrum of  $-2.7$ . The zenith angles of primary protons are  $0^\circ$  (vertical showers) and  $30^\circ$  (inclined showers). The lowest energy cutoff for  $e^\pm$  and  $\gamma$  in our simulations is set to 0.05 MeV. This means that electrons below this energy are discarded before they may be accelerated to higher energies by the electric field.

In our simulation work, we assume the electric fields uniformly distribute from 5400 m to 4400 m (corresponding to the atmospheric depth from 457 g/cm<sup>2</sup> to 599 g/cm<sup>2</sup>). The values of the geomagnetic field components used in simulations are  $B_X = 34.6 \mu\text{T}$ ,  $B_Z = 35.7 \mu\text{T}$ , corresponding to the horizontal and vertical intensity, respectively. It can be calculated that the value of runaway electric field of the detection surface (LHAASO observatory) is 1660 V/cm according to the formula proposed by Dwyer[5]. For studying the effects of thunderstorm electric fields with different intensities on the lateral distribution of secondary particles, we chose two typical electric fields (-1000 V/cm and -1700 V/cm) in this work.

### 3. Simulation results

Here, we show the electric effects on lateral distribution of vertical and inclined showers.

#### 3.1 The lateral distribution of $e^\pm$ and $\gamma$ in absence of electric field.

In order to better understand the lateral distribution of secondary particles in cosmic ray, we simulate the case without electric field firstly.

Fig.1 shows the density distribution of  $e^\pm$  and  $\gamma$  for vertical shower ( $\theta = 0^\circ$ ) as a function of distance to shower core in absence of an electric field. As shown in the Fig.1, we can know that the density of photons far exceeds the total density of the positrons and electrons. The corresponding distributions are normalized to the density at 2000 m of distance from the shower core (shown in Fig. 2). We can see that the lateral distribution of  $\gamma$  is wider than that of  $e^\pm$ .

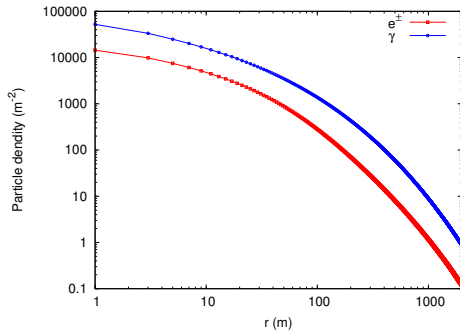


**Fig. 1:** The particles density for vertical showers as a function of distance to shower core without electric field.

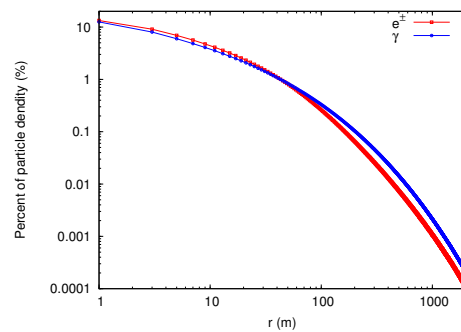


**Fig. 2:** Lateral distributions (normalized at 2000m) for vertical showers without electric field.

The results for inclined showers ( $\theta = 30^\circ$ ) are plotted in Fig.3 and Fig.4. From the following figures, we can see that the density of photons is much higher than the total density of the positrons and electrons. In addition, the laws of particles density for inclined showers is almost the same as that of vertical showers.

The average lateral radius  $\bar{r}$  are analyzed to better study the lateral distribution characteristics of the secondary particles in the extensive air shower(EAS). It is defined as follows:

$$\bar{r} = \frac{\sum r_i}{N} \quad (1)$$

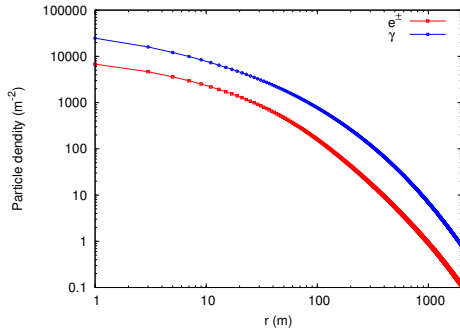


**Fig. 3:** The particles density for inclined showers as a function of distance to shower core without electric field.

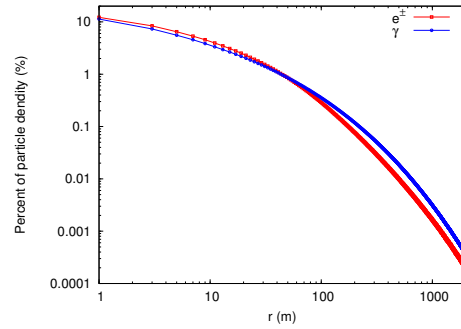
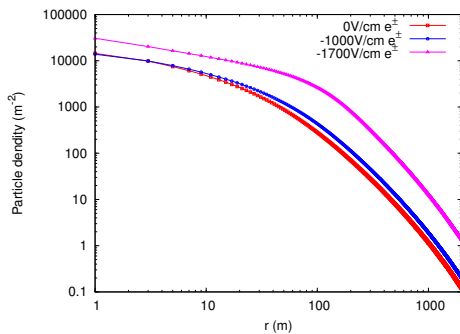


**Fig. 4:** Lateral distributions (normalized at 2000m) for inclined showers without electric field.

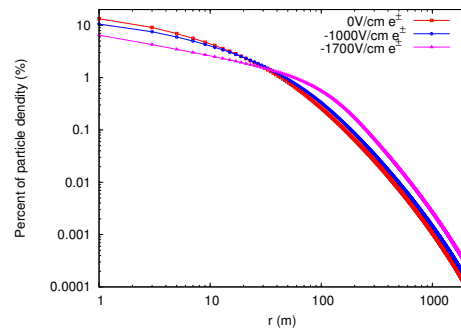
Here  $r_i$  is the distance of the particle  $i$  to shower core at detector level,  $N$  is the total number of particles in the showers. According to the above formula, we can calculate the average radius of  $e^\pm$  and  $\gamma$  for vertical showers is 272 m and 345 m, respectively. As for inclined showers, the average radius of  $e^\pm$  and  $\gamma$  is 321 m and 396 m. We can know that the lateral distribution of inclined showers is wider than that of vertical showers.

### 3.2 Lateral distribution of vertical showers in different electric fields.

In order to see the change of the particle density under the electric fields more clearly, we also draw the simulation results without electric field in the following figures. The total density distribution of  $e^\pm$  for vertical shower as a function of distance to shower core in different electric fields and the corresponding normalized one are shown in Fig.5 and Fig.6, respectively. As we can see from the two figures that the lateral distribution of  $e^\pm$  is larger in the presence of electric fields, especially in the electric field of -1700 V/cm. In addition, the enhanced amplitude of particle density is much larger away from the shower core while that is small in the range near shower core, even it may decrease in -1000 V/cm. It can be calculated that the average radius of  $e^\pm$  is 336 m in -1700 V/cm and 290 m in -1000 V/cm.



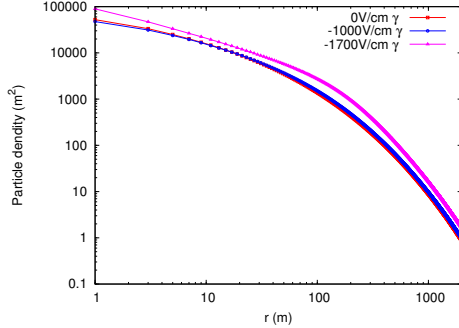
**Fig. 5:** The particle density of  $e^\pm$  for vertical showers as a function of distance to shower core in -1000 V/cm and -1700 V/cm.



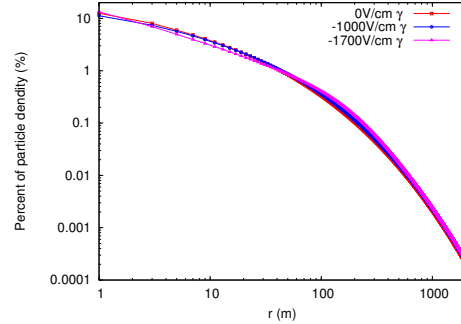
**Fig. 6:** Lateral distribution of  $e^\pm$  (normalized at 2000m) for vertical showers in -1000 V/cm and -1700 V/cm.

Fig.7 and Fig.8 show the lateral distribution of photons for vertical showers in the different electric fields, respectively. What we can see from the following figures is that the density of

photons is almost the same in electric fields, but it has changed greatly in the electric field of -1700 V/cm. It can be calculated that the average radius of photons is 351 m in -1700 V/cm and 347 m in -1000 V/cm.



**Fig. 7:** The particles density of  $\gamma$  for vertical showers as a function of distance to shower core in -1000 V/cm and -1700 V/cm.



**Fig. 8:** Lateral distribution of  $\gamma$  (normalized at 2000m) for vertical showers in -1000 V/cm and -1700 V/cm.

### 3.3 Lateral distribution for inclined showers in different fields.

Fig.9 and Fig.10 show the total density of  $e^\pm$  for inclined shower and the corresponding normalized density in -1000 V/cm and -1700 V/cm, respectively. We can draw two conclusions from the figures, one is that the  $e^\pm$  density decreases with small distance to shower core, but increases obviously with large core distance; the other is that change amplitude is much larger in -1700 V/cm. That is to say that the lateral distribution of positrons and electrons is increased with the electric field intensity. The average radius of positrons and electrons is 506 m in -1700 V/cm and 349 m in -1000 V/cm.

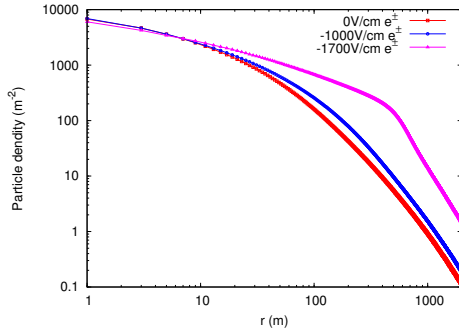


**Fig. 9:** The particle density of  $e^\pm$  for inclined showers as a function of distance to shower core in -1000 V/cm and -1700 V/cm.

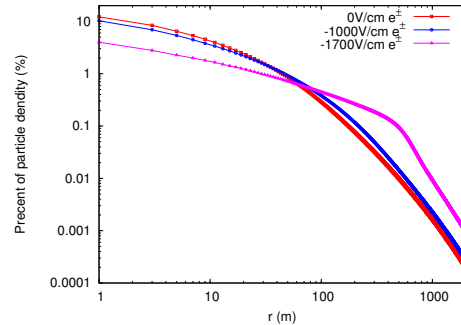


**Fig. 10:** Lateral distribution of  $e^\pm$  (normalized at 2000m) for inclined showers in -1000 V/cm and -1700 V/cm.

Fig.11 and Fig.12 show the density of photons for inclined showers and the corresponding normalized density under the same conditions, respectively. As we can see that the density and lateral distribution of photons are hardly change in -1000 V/cm. However, the change is obvious in the electric field of -1700 V/cm. The density of photons decreases near the shower core, while increases far away from the shower core. It can be calculated the mean lateral radius of photons for inclined showers is 481 m in -1700 V/cm and 402 m in -1000 V/cm.

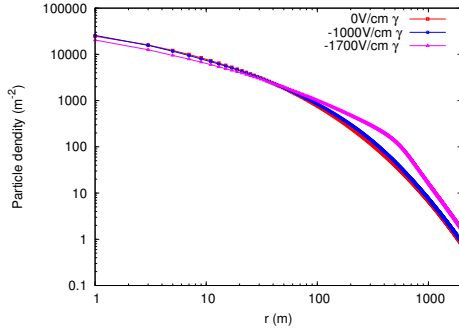


**Fig. 11:** The particle density of  $\gamma$  for inclined showers as a function of distance to shower core in -1000 V/cm and -1700 V/cm.

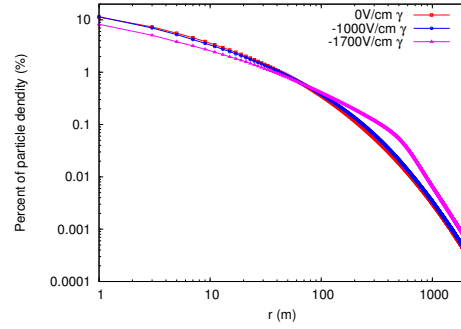


**Fig. 12:** Lateral distribution of  $\gamma$  (normalized at 2000m) for inclined showers in -1000 V/cm and -1700 V/cm.

#### 4. Discussion

From the above analysis, we can know that the lateral distribution of positrons, electrons and photons is larger during thunderstorm. Moreover, the variation amplitude is dependent on electric field intensity and direction of the shower events.

The average radius with different primary zenith angles in different electric fields are listed in table 1. We can see that the enhanced amplitude of  $e^\pm$  for vertical shower reaches 6.6% in -1000 V/cm and 23.5% in -1700 V/cm and that of photons are 0.6% and 1.7%, respectively. For a zenith angle of 30 degrees, the enhanced amplitude of  $e^\pm$  reaches 8.7% in -1000 V/cm and 57.6% in -1700 V/cm and that of photons are 1.5% and 21.4%, respectively. That means that average radius of inclined showers is larger than that of vertical shower and the variation amplitude during thunderstorms is larger than the one of vertical showers. In addition, we can draw a conclusion that the average radius increases with the electric field and the enhanced amplitude of electrons and positrons becomes larger, especially in -1700 V/cm.

**Table 1:** The average radius  $\bar{r}$  in different fields with different primary zenith angles

Electric field (V/cm)	$\bar{r}_{\theta=0^\circ}(e^\pm)$	$\bar{r}_{\theta=0^\circ}(\gamma)$	$\bar{r}_{\theta=30^\circ}(e^\pm)$	$\bar{r}_{\theta=30^\circ}(\gamma)$
0	272	345	321	396
-1000	290	347	349	402
-1700	336	351	506	481

During thunderstorms, the lateral distribution of positrons, electrons and photons will be wider and the variation amplitude of positrons and electrons is larger than that of photons. As known to all that the charged particles will acceleration or deceleration in thunderstorm electric field [10]. To explain our simulation results reasonably, we plotted the corresponding energy of secondary particles as a function of distance to shower core in Fig.13 and the average energy of particles with different electric fields is calculated in Table 2. We can know that the secondary particles with larger energy is closer to the shower core, while smaller energy far from the shower core. A large number of electrons with small energy are biased away from the shower core due to the deflection of negative electric field on secondary particles. The simulation result indicated that the effect of

negative electric field on electron is more obvious than that of positron [11]. In addition, the photons in secondary cosmic rays are mainly produced by bremsstrahlung [7]. Therefore, the thunderstorm field as well as has a secondary effect on the photons. As a result, the density of positrons, electrons and photons increases synchronously in thunderstorms.

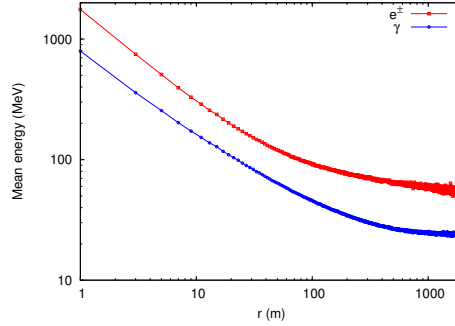


**Fig. 13:** The mean energy of secondary particles for vertical showers without electric field.

**Table 2:** The average energy in different fields with different primary zenith angles

Electric field (V/cm)	$\bar{E}_{\theta=0^\circ}$ (MeV) ( $e^\pm$ )	$\bar{E}_{\theta=0^\circ}$ (MeV) ( $\gamma$ )	$\bar{E}_{\theta=30^\circ}$ (MeV) ( $e^\pm$ )	$\bar{E}_{\theta=30^\circ}$ (MeV) ( $\gamma$ )
0	104	43	99	41
-1000	72	40	69	38
-1700	22	28	19	23

As shown in Figs.10-12, we can know that the lateral distribution of secondary particles for inclined showers is wider than that for vertical showers during thunderstorms. We can also see from Table 2 the mean energy of secondary particles for inclined showers is smaller than that of vertical showers. Thus, the effect of electric field on secondary particles for inclined showers is more obvious. The study found that the thickness of the atmospheric layer increases with the zenith angle [12, 13]. Therefore, the atmosphere for an inclined shower is less dense at the same slant depth [14, 15]. In a region of low density, the lost energy of particles due to collisions is smaller and acceleration in the electric field is more efficient.

## 5. Conclusion

In this paper, Monte Carlo simulations were performed to study the effects of near-earth thunderstorms electric field on the lateral distribution of vertical and inclined showers at LHAASO observatory. We found the lateral distribution of secondary particles is closely related to strength of electric field and direction of the shower event.

The lateral distribution of positrons, electrons and photons widens in thunderstorm electric fields while the amplitude of photons is smaller than that of positrons and electrons. The variation amplitude of lateral distribution increases with the strength of electric field. Our simulation results as well as show that the variation for inclined showers is larger than that of vertical showers.

Our simulation results could provide important information for reconstructing the shower core and primary arrival direction. It is also useful to study the acceleration mechanism of secondary charged particles caused by an atmospheric electric field.

### **Acknowledgments**

This work is supported by the National Natural Science Foundation of China (NSFC) under Grants No. U2031101, 11475141 and 12047576.

### **References**

- [1] K.G. Axi, et al., In: Proceedings of 36th ICRC, Madison, USA, July 24 August 1, 496 (2019).
- [2] F. Aharonian, et al. (LHAASO Collaboration), *Chinese Phys. C* 45, 025002 (2021).
- [3] H. Wang, et al., *Phys. Nuc.* 27, 299-303 (2003).
- [4] D.R. MacGorman, et al., Oxford Univ. Press, New York. 70, 560 (1998).
- [5] R.C.T. Wilson, *Proc. Phys. Soc.* 37 (1924) 32D-37D London.
- [6] A.V. Gurevich, et al., *Phys. Lett. A* 165, 463-468 (1992).
- [7] B. Zhao, et al., In: Proceedings of 36th ICRC, Madison, USA, July 24 August 1, 289 (2019).
- [8] Z. Cao, et al., *Acta Astronom. Sin.*, 43, 457-478 (2019).
- [9] D. Heck, et al., FZKA:Forschungszentrum Karlsruhe GmbH, Karlsruhe, 6019, 1998.
- [10] X.X. Zhou, et al., *Astropart. Phys.* 84, 107-114 (2016).
- [11] R.R. Yan, et al., *Chin. Astron. Astr.* 44, 146-159 (2020).
- [12] A. Bhadra, *Pramana-J. Phys.* 52, 133-144 (1999).
- [13] X.X. Zhou, et al., *Acta Phys. Sin.* 64, 405-412 (2015).
- [14] S. Buitink, et al., *Astropart. Phys.* 33, 1-12 (2010).
- [15] B. Bartoli, et al. (ARGO-YBJ Collaboration), *Astropart. Phys.* 93, 46-55 (2017).